An X-Ray Diffraction Study on the Structure of Concentrated Aqueous Caesium Iodide and Lithium Iodide Solutions

Yusuke Tamura, Toshio Yamaguchi *, Isao Okada, and Hitoshi Ohtaki
Department of Electronic Chemistry, Tokyo Institute of Technology, Nagatsuta, Midori-ku, Yokohama 227, Japan

Z. Naturforsch. **42 a**, 367–376 (1987); received December 8, 1986

X-Ray scattering measurements of 2.78 and 5.56 molal aqueous solutions of caesium iodide and 2.78 and 6.05 molal lithium iodide were carried out at 293 and 343 K. Differences in the radial distribution functions (DRDFs) have been obtained between the caesium iodide and lithium iodide solutions of similar composition, the latter being taken as a reference for the data analysis of the former. The DRDFs show a peak arising from Cs–I contact-ion-pairs at 390 pm for all the caesium iodide solutions. The hydration structure of the caesium and iodide ions has been revealed. Effects of the concentration and temperature on the formation of ion-pairs and on the hydration structure of the ions are discussed.

1. Introduction

The structure of electrolyte solutions, in particular alkali halide solutions, has widely been investigated by means of X-ray and neutron diffraction [1] and Monte Carlo and molecular dynamics simulations [2], from which the structure and properties of hydrated ions have been revealed. However, almost all of these studies are limited to the systems at room temperature.

The temperature dependence of the structure of hydrated ions in aqueous solution has extensively been investigated by NMR [3, 4], conductivity [5], thermochemical measurements [6, 7], neutron scattering [8], and density measurements [9]. From these it has been concluded that ions which display negative hydration at room temperature change to positive hydration with increasing temperature at a so-called cross-over temperature. Buslaeva and Samoilov [10] examined the temperature dependence of the hydration number of alkali metal and halide ions in dilute solutions by a thermochemical method, the results showing that with an increase in temperature the hydration number of these ions except Li^+ increases. However, the above studies have given only indirect information with respect to structural properties of hydrated ions. Recently, Heinzinger *et al.* have obtained direct structural information on the effect of temperature and pressure on the hydration shells of Li^+ and I^- and on the bulk water by means of molecular dynamics (MD) simulations of a 0.55 molal LiI solution at 308 and 508 K [11].

Ionic association is another essential factor in understanding the physico-chemical properties of concentrated alkali halide solutions. The formation of ion-pairs in aqueous alkali halide solutions has been predicted on the basis of thermodynamic data [12, 13]. The first direct evidence of contact-ion-pairs has been obtained by Lawrence and Kruh [14] from their X-ray diffraction studies of concentrated alkali solutions. Among the solutions of LiCl, LiBr, LiI, NaI, CsCl, CsBr and CsI they found contact-ion-pairs only in the caesium salts solutions. In X-ray measuremets of concentrated aqueous KI solutions, Fishkis and Soboleva [15] reported the formation of $K^+–I^-$ ion-pairs. Szász and Heinzinger [16] discussed the formation of short lived $Cs^+–F^-$ ion-pairs formed in a 2.2 molal aqueous CsF solution from an MD simulation. Neutron diffraction studies on concentrated aqueous LiCl solutions have revealed that $Li^+–Cl^-$ contact-ion-pairs are formed [17, 18]. A recent MD simulation has also shown the formation of $Li^+–Cl^-$ pairs in an aqueous LiCl solution having the $[H_2O]/[LiCl]$ molar ratio of four [19]. In

Reprint requests to Prof. H. Ohtaki, Department of Electronic Chemistry, Tokyo Institute of Technology, Nagatsuta, Midori-ku, Yokohama 227, Japan.
* Present address: Department of Chemistry, Faculty of Science, Fukuoka University, Nanakuma, Jonan-ku, Fukuoka 814-01, Japan.

0340-4811 / 87 / 0400-0367 $ 01.30/0. – Please order a reprint rather than making your own copy.

an aqueous solution with the $[H_2O]/[LiCl]$ molar ratio of 3 (18.5 molal), more extensive ion-pair formation between Li^+ and Cl^- ions has been revealed by both X-ray diffraction experiment and MD simulations [20, 21]. To our knowledge, no investigation on ion-pair formation has yet been carried out in aqueous alkali halide solutions at elevated temperatures.

In the present paper, we report the results of X-ray diffraction studies on aqueous 2.78 and 6.05 molal LiI solutions and 2.78 and 5.56 molal CsI solutions at different temperatures. The ions Li^+ and Cs^+ were chosen in order to see the difference of ionic size.

2. Experimental

Commercially available caesium iodide (min. 99.5%) was recrystallized once from water, and reagent grade lithium iodide was used without further purification. The concentrations of the solutes were determined by gravimetry of iodide ions using an $AgNO_3$ solution. The densities of the solutions were measured at 293 and 343 K by the pycnometric and Archimedes methods, respectively. Data of the sample solutions are given in Table 1. Solutions E and G are almost saturated at 293 and 343 K, respectively.

A $\theta-\theta$ diffractometer was used with Mo$K\alpha$ radiation ($\lambda = 71.07$ pm) for the X-ray diffraction measurements. The measured range of the scattering angle (2θ) was $2-140°$, corresponding to an s-range of $0.003-0.16\ \mathrm{pm}^{-1}$ ($s = 4\pi \sin\theta/\lambda$). At angles θ below 1° the measured intensities were linearly extrapolated to zero at $\theta = 0°$. 80 000 counts at each data point were accumulated in the whole scan range. The diffractometer and details of data collection have been described in [22]. Corrections for absorption, polarization, double scattering and incoherent scattering, and subsequent scaling of the corrected scattering intensities to the electron units were carried out in the same way as previously described [22, 23].

The structure function $i(s)$ is obtained by subtracting the independent scatterings from all atoms in the sample solutions from the scaled intensities $I(s)$:

$$i(s) = I(s) - \sum x_i f_i(s)^2 , \tag{1}$$

where x_i is the number of the i-th atom in the stoichiometric volume V containing one iodine atom and $f_i(s)$ is the coherent scattering factor corrected for the real and imaginary parts of the anomalous dispersion. The coherent and incoherent scattering factors of neutral atoms were taken from the International Tables [24]. The structure functions multiplied by the scattering vector s of the sample solutions are shown in Figs. 1 a and 2 a for the LiI and CsI solutions, respectively.

The radial distribution function (RDF) is calculated by the Fourier transform of the structure function:

$$D(r) = 4\pi r^2 \varrho_0 + \frac{2r}{\pi} \int_0^{s_{max}} s\, i(s)\, M(s) \sin(sr)\, \mathrm{d}s , \tag{2}$$

where ϱ_0 is the average electron density in the stoichiometric volume V containing one iodine atom, and s_{max} is the maximum s-value attained in the measurements. A modification function, $M(s)$, with regard to one iodine atom, of the form $[f_I(0)^2/f_I(s)^2] \exp(-100\, s^2)$ was applied to all of the structure functions in common.

The synthetic structure function based on a model is obtained by

$$i(s)_{syn} = \sum\sum x_i n_{ij} f_i f_j \frac{\sin(s r_{ij})}{s r_{ij}} \exp(-b_{ij} s^2) - \sum\sum x_i x_j f_i f_j \frac{4\pi R_j^3}{V} \frac{\sin(sR_j) - sR_j \cos(sR_j)}{(sR_j)^3} \cdot \exp(-B_j s^2) . \tag{3}$$

Table 1. Concentrations (mol/kg H_2O), water/salt molar ratios, densities (g/cm^3), and temperatures (K) of the sample solutions.

Solution	LiI	$[H_2O]/[LiI]$	d	T	Solution	CsI	$[H_2O]/[CsI]$	d	T
A	2.78	20.0	1.25	293	E	2.78	20	1.47	293
B	2.78	20.0	1.22	343	F	2.78	20	1.44	343
C	6.05	9.19	1.49	293	G	5.56	10	1.79	343
D	6.05	9.19	1.45	343					

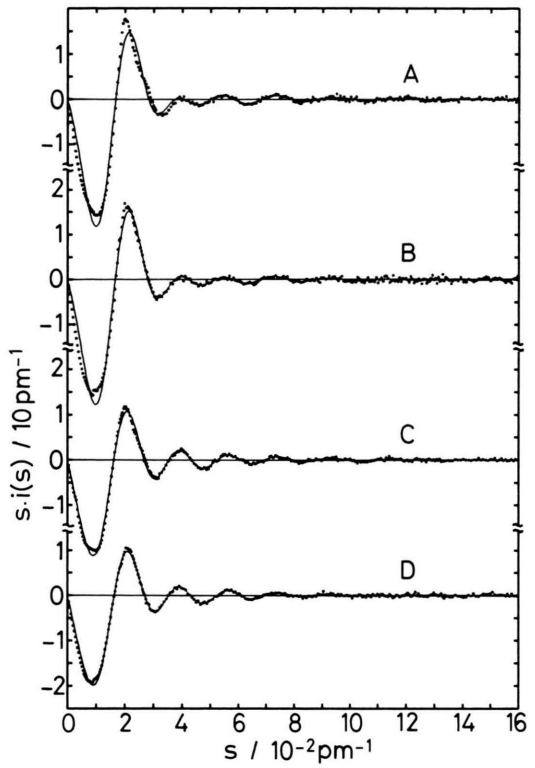

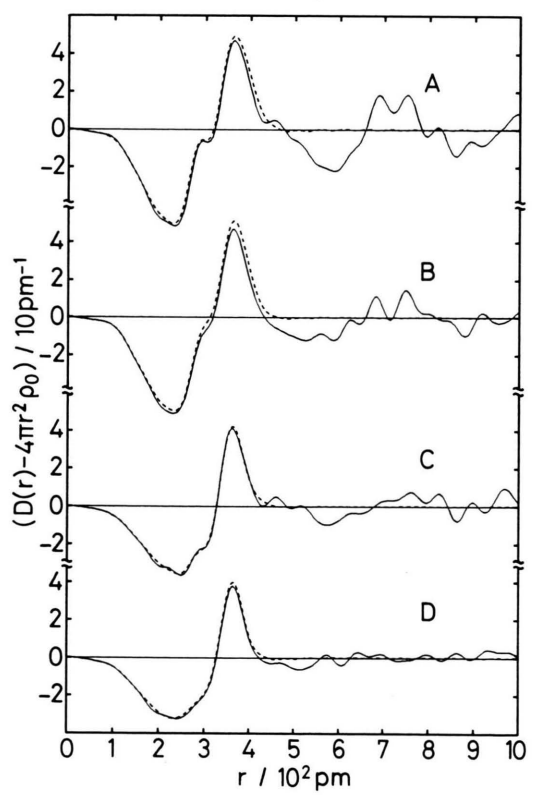

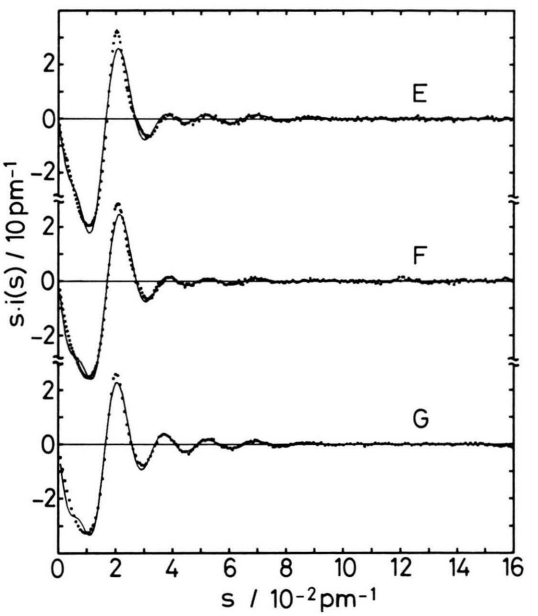

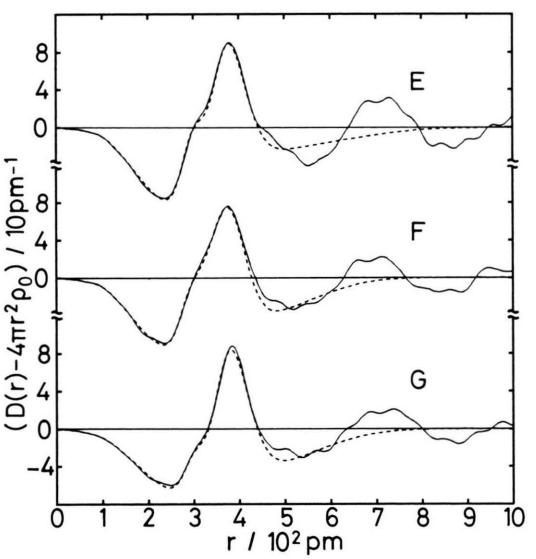

Fig. 2. a) Structure functions of the aqueous CsI solutions: experimental (dots) and calculated (solid lines). b) Radial distribution functions in the form of $D(r) - 4\pi r^2 \varrho_0$ of the aqueous CsI solutions: experimental (solid lines) and calculated (dashed lines).

Fig. 1. a) Structure functions of the aqueous LiI solutions: experimental (dots) and calculated (solid lines). b) Radial distribution functions in the form of $D(r) - 4\pi r^2 \varrho_0$ of the aqueous LiI solutions: experimental (solid lines) and calculated (dashed lines).

Table 2. Parameter values used for the model calculations on the LiI solutions of Fig. 1: the interatomic distance r (pm), the temperature factor $10b$ (pm^2), the number of interactions n, and the parameters of the continuum electron distribution R (pm) and $10B$ (pm^2). The values in parentheses are their standard deviations estimated from the least-squares fits. The parameter values without parentheses were fixed during the calculations.

		A 2.78 molal 293 K	B 2.78 molal 343 K	C 6.05 molal 293 K	D 6.05 molal 343 K
Li–O	r	220(8)	–	228(3)	–
	$10b$	10	–	10	–
	n	4	–	4	–
I–O	r	357.7(5)	358.2(2)	355.0(2)	359.1(2)
	$10b$	46(2)	33.8(5)	18.5(4)	16.4(3)
	n	8.3(1)	7.73(4)	5.58(5)	4.72(3)
O–O	r	279.9(4)	286.9(3)	283.2(4)	280(1)
	$10b$	8.3(7)	7.0(4)	5.8(5)	21(2)
	n*	3.39(4)	2.27(2)	2.34(3)	1.63(4)
Li	R	450(30)	330(20)	330(10)	290(30)
	$10B$	10	10	10	10
I	R	394(2)	385(1)	380(1)	363(1)
	$10B$	21(7)	29(4)	34(2)	84(5)
H	R	297(4)	242(3)	288(3)	234(4)
	$10B$	30(20)	80(20)	40(20)	10(20)
O	R	316(1)	301(1)	311(1)	286(1)
	$10B$	46(4)	87(3)	100(4)	92(5)

* Per H_2O molecule.

The first term of the right-hand-side of (3) is related to short-range interactions characterized by the interatomic distance, r_{ij}, the temperature factor, b_{ij}, and the number of interactions, n_{ij}, for atom pairs $i-j$. The second term arises from the interaction between a spherical hole and the continuum electron distribution beyond this discrete distance. R_j is the radius of the spherical hole around the j-th atom and B_j the softness parameter for emergence of the continuum electron distribution. All the calculations were carried out by means of the programme KURVLR [25].

3. Results and Discussion

3.1. Radial Distribution Functions (RDFs)

3.1.1. RDFs of Lithium Iodide Solutions

Figure 1 b shows the radial distribution functions in the form $D(r) - 4\pi r^2 \varrho_0$ for the four LiI samples of Table 1.

In all the RDFs a pronounced peak appeared at 370 pm, which was ascribable to the I–O interactions within the first hydration shell of the iodide ion from the sum of the effective radius of I^- and H_2O. The position of the peak corresponds well to that found in other X-ray diffraction studies of aqueous iodide solutions [14, 15, 26–29].

In the RDF of the 2.78 molal solution at 293 K (Fig. 1 b, A) a small peak appeared around 290 pm, which is due to the first neighbour H_2O–H_2O interactions in the bulk water and also the interactions between the water molecules coordinated to Li^+ and I^- and the hydrogen-bonded water molecules in the second coordination shell. Only a shoulder was observed around 290 pm in solution C with its high concentration of the solute. When the temperature increased, the shoulder became broader (Fig. 1 b, B) and practically disappeared in the solution of the highest concentration and temperature (Fig. 1 b, D).

The RDFs show complex features in the range 400–600 pm which change with concentration and temperature. The RDF of sample A may be characterized by a peak at 450 pm, a shoulder around 500 pm and a deep minimum around 580 pm. This feature is in good agreement with that found for a 2.2 molal LiI solution reported by Radnai *et al.* [29].

When the temperature increased (sample B), the peak and the shoulder disappeared, the minimum around 580 pm became shallower and a new peak appeared around 550 pm. When the solute concentration increased to 6.05 molal (sample C), two peaks appeared at 450 and 520 pm and the minimum around 550 pm became shallower. With increasing temperature the features observed for solution C were reduced, while a new peak appeared at 570 pm.

The above characteristic changes in the RDFs may correspond to the findings from MD simulations of a 2.2 molal LiI solution at 305 K [28] and of a 0.55 molal LiI solution at 308 and 508 K [11]. The second peak in the O–O pair correlation function of the 2.2 molal LiI solution splitted into two at 430 and 520 pm, in contrast to a single broad peak at 460 pm found in pure water. Furthermore, in the ion-oxygen pair correlation functions, the second nearest-neighbour ion-water interactions appeared around 420 and 520 pm for Li^+ and I^-, respectively. Thus, the two peaks around 450 and 520 pm observed for sample A are ascribable to the H_2O-H_2O interactions and in part to the second nearest-neighbour ion-water interactions. A comparison between the O–O pair correlation functions at 308 and 508 K for the 0.55 molal LiI solution [11] indicates that the second peak appearing around 460 pm at 308 K shifts to a longer distance of 560 pm at 508 K. This shift well explains the appearance of the new peak around 560 pm in our samples. Thus, the peak around 560 pm observed for the two LiI solutions at 343 K may arise from the H_2O-H_2O interactions. The MD simulation has also shown a broadening of the peaks arising from the second neighbour ion-water interactions with increasing temperature, such broadening being also seen for the peak around 460 pm in our sample D.

With respect to the cation hydration, the first neighbour Li–O distance has been reported to be 195–220 pm in the literature [1]. In the present study, because of the small X-ray scattering power of Li, the corresponding peak cannot be seen in the RDF of the 2.78 molal solution, but a small peak is discernible around 210 pm for the 6.05 molal solution at 293 K.

3.1.2. RDFs of Caesium Iodide Solutions

As can be seen in Fig. 2 b, the RDFs of all the CsI solutions show a shoulder around 300 pm, a distinct peak at 380 pm and a broad peak at 600–800 pm.

The first neighbour H_2O-H_2O interactions, which usually appear at about 280 pm for aqueous solutions [22, 23, 30], may in part contribute to the shoulder around 300 pm. Also the interactions between Cs^+ and the water molecules in the first hydration shell should be responsible for the shoulder as expected from the findings in other X-ray diffraction studies of aqueous solutions of caesium salts [14, 31] and from the sum of the effective radius of Cs^+ (169 pm) and H_2O (140 pm).

The peak at 385 pm should partly originate from the $I^- - H_2O$ interactions due to hydrated I^- ions, which appear around 360 pm, as seen in the RDFs of the LiI solutions (Fig. 1 b). However, the main peak observed for the CsI solutions is shifted to a longer distance by about 20 pm from that for the LiI solutions. This shift of the distance is beyond experimental errors and thus indicates the presence of another interaction around 385 pm in the CsI solutions.

In order to separate the peaks due to the $Cs^+ - H_2O$ interactions and an unknown interaction superimposed on the peak at 385 pm, we employed the procedure proposed by Lawrence and Kruh [14]. Since all the RDFs of the aqueous CsI and LiI solutions are normalized to the stoichiometric volume containing one I^- ion in the present study, the CsI and LiI solutions at a similar ion concen-

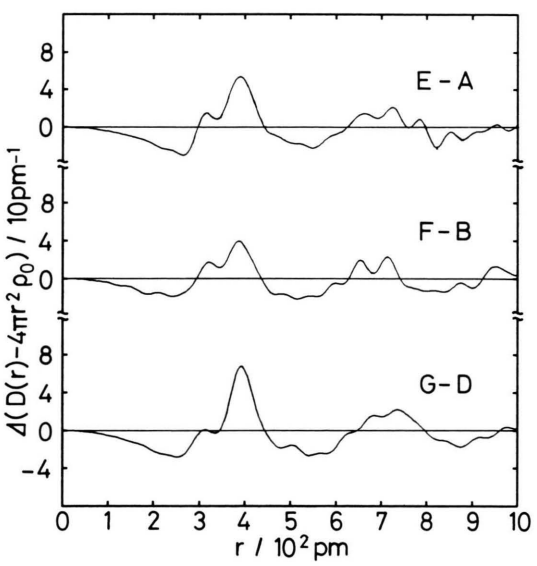

Fig. 3. The difference in the radial distribution functions obtained from the RDFs shown in Figs. 1 b and 2 b.

tration contain almost the same number of water molecules. Therefore, the RDFs for the CsI and LiI solutions of the same composition and temperature should give peaks of the same shape which arise from the first neighbour H_2O-H_2O interactions and the I^--H_2O interactions. Accordingly the difference in the radial distribution functions (DRDFs), obtained by subtracting the RDFs of the LiI solutions from those of the CsI solutions of the corresponding composition and temperature may yield better information about the Cs^+-H_2O interaction and another one hidden in the peak at 385 pm.

As seen in Fig. 3, the resulting DRDFs have revealed two peaks at 310 and 385 pm. The former peak can be assigned to the Cs^+-H_2O interactions, the distance of which is in good agreement with the previous findings from X-ray investigations of caesium salt solutions [14, 31]. Since the position of the latter peak is essentially the same as the sum of the effective ionic radii of Cs^+ and I^- (169 + 216 = 385 pm), the peak should be ascribed to directly contacted Cs^+-I^- ion-pairs formed in the CsI solutions.

All the DRDFs have shown a large broad peak centred around 700 pm, which has not been observed for the LiI solutions (Figure 1 b). This peak could not be assigned to the secondary Cs^+-H_2O nor I^--H_2O interactions since, according to the MD simulations of 2.2 molal aqueous LiI and CsF solutions [11, 16, 28], the broad second peaks appear at 500–600 pm in the Cs–O and I–O pair correlation functions. If we assumed that the cations and anions were uniformly distributed in the CsI solutions, the average distances for the cation-cation, anion-anion, and cation-anion pairs could be estimated to be about 700 pm. An alternative assignment of this broad peak is based on the formation of aggregates such as $I^--Cs^+-I^-$ or $Cs^+-I^--Cs^+$ in the CsI solutions, since the distance of non bonding I ... I and Cs ... Cs interactions could fall within the range 600–800 pm, depending on the $I^--Cs^+-I^-$ and $Cs^+-I^--Cs^+$ angles. In both cases the expected interatomic distance between the ions could fit the position of the broad peak found for the CsI solutions.

3.2. *Models*

In order to determine the values of the structural parameters of the hydrated ions, the experimental structure functions were compared with theoretical ones of models obtained by use of (3). For this purpose a non-linear least-squares fitting procedure was employed, in which the function

$$U = \sum_{s_{\min}}^{s_{\max}} w(s)\,[i_{\exp}(s) - i_{\mathrm{syn}}(s)]^2 \qquad (4)$$

was minimized with respect to variables r_{ij}, b_{ij}, n_{ij}, R_j, and B_j by using the programme NLPLSQ [32]. Here, $s_{\min}$ and $s_{\max}$ are the lower and upper limits of s, respectively, used in the calculations, and $w(s)$ is the weighting function of s^4.

In the X-ray scattering study of a 2.2 molal LiI solution, Radnai *et al.* [29] assumed a model for the Li^+ hydration, in which both the first and second coordination shells of Li^+ were taken into account. In the present system, however, the RDFs at $r = 450-500$ pm have changed in a complicated manner with changes in temperature and concentration. Thus, we approximated interactions longer than 400 pm in terms of the continuum electron distribution around each atom; thereby contributions of the long-range interactions to the I–O peak at 360 pm might be treated in a similar manner for all the sample solutions. The model for LiI solutions adopted here as the following characteristics:

a) The hydration of Li^+ is defined by the first neighbour Li–O distance, the corresponding temperature factor and the hydration number. According to the previous neutron diffraction [1] and the MD simulation [2], the average hydration number of Li^+ ion changes from four to six, depending on the ion concentration. In the present case, two values, four and six, for the hydration number of Li^+ ion were examined for the sake of simplicity, and the geometry of the hydration shell was assumed to be tetrahedral for the former and octahedral for the latter case. The H_2O-H_2O interactions within the coordination shell were also taken into account in terms of the interatomic distance r'_{OO}, the temperature factor b'_{OO}, and the number of interactions n'_{OO}. The symmetry was held in the course of the calculations.

b) The hydration of I^- is expressed in terms of the distance r_{IO}, the temperature factor b_{IO} and the coordination number n_{IO}. These parameters were allowed to vary independemtly. Since the H_2O-H_2O interactions in the hydration shell of I^- were ex-

pected to have the O−O distance of 500−600 pm, where we assumed the continuous electron distribution, we did not estimate the structural parameters of the H_2O-H_2O interactions within the hydration shell of I^-.

c) The nearest H_2O-H_2O contacts in the bulk water, as well as those between the first and second hydration shells of Li^+ and I^-, were characterized in terms of the distance r_{OO}, the temperature factor b_{OO} and the number of interactions n_{OO}, which were varied independently in the fitting procedure.

d) Beyond the distance $r > 400$ pm, a uniform electron distribution was assumed around each atom by introducing parameters R_j and B_j in (3).

On the basis of the assignments of the peaks in the RDFs stated in the preceding section, the following model was examined for the CsI solutions:

a) The structures of the first hydration shells of Cs^+ and I^- were taken into account, which were described in terms of interatomic distances (r_{CsO}, r_{IO}), temperature factors (b_{CsO}, b_{IO}), and the number of water molecules in the hydration shells (n_{CsO}, n_{IO}). This assumption seemed reasonable since the second hydration shells of both ions have been found not to be structurally well ordered according to the MD simulations of 2.2 molal aqueous CsF and LiI solutions [11, 16, 28]. The above six parameters were allowed to vary independently. The H_2O-H_2O interactions in the first hydration shells of Cs^+ and I^- were not taken into account for the following reason: if Cs^+ had a regular polyhedral hydration shell with the Cs−O distance experimentally obtained, the H_2O-H_2O interactions with the hydration shell would appear at the distance predicted from the polyhedral structure. For instance, if the structure of hydrated Cs^+ were tetrahedral, the O−O distance would be about 500 pm ($= 305$ pm $\times \sqrt{8/3}$), and if it were octahedral, the O−O distance would become ≈ 430 pm ($= 305$ pm $\times \sqrt{2}$), and so on. However, no appreciable peak has been observed in this region in the RDFs. A similar consideration may be made for the H_2O-H_2O interactions within the hydration shell of I^-. Therefore, we concluded that these rather weakly hydrated ions have hydration shells in which the water molecules are practically randomly situated. This agrees with the considerations from the MD simulation by Szász *et al.* [11, 16, 28].

b) The contacted Cs^+-I^- ion-pairs are characterized by the interatomic distance r_{CsI}, the temperature factor b_{CsI}, and the number of interactions n_{CsI}. The parameter n_{CsI} was independently refined, since a formation of aggregates of the ions could not be ruled out in the CsI solutions, as discussed in the preceding section.

c) The first neighbour H_2O-H_2O interactions, which should be present in aqueous solutions, were introduced by using the interatomic distance r_{OO}, the temperature factor b_{OO}, and the number of interactions n_{OO} as adjustable parameters.

d) Beyond the above discrete interactions the continuum of electron distribution was assumed for all the atoms.

The s range used was $0.001-0.16$ pm^{-1} for both the LiI and CsI solutions. The final results are summarized in Tables 2 and 3 for LiI and CsI solutions, respectively. Figures 1 and 2 show that the theoretical curves reproduce well those observed.

3.3. Li^+ Hydration

In order to judge the reliability of the model we used a factor R, which is similar to the one usually employed in crystallography.

$$R^2 = \frac{\sum w(s)\{i_{exp}(s) - i_{syn}(s)\}^2}{\sum w(s)\, i_{exp}(s)^2}. \qquad (5)$$

Among the two (tetrahedral and octahedral) models assumed above, their R-values did not differ significantly from each other due to a small contribution of the structure function of hydrated Li^+ to the whole one. Thus, a definite conclusion was not obtained for the concentration and temperature dependence of the hydration of Li^+ from the present investigation. Therefore, we tentatively assumed that Li^+ had the four-coordinated structure in the present case. The assumption of the six-coordinaion structure gave a similar result.

The effect of ion concentration and temperature on the hydration structure of Li^+ has been examined by means of neutron diffraction, which will be published elsewhere [33].

3.4. Cs^+ Hydration

As seen in Table 3, the average hydration number for Cs^+ decreases with increasing concentration.

Table 3. Results of the least-squares fits obtained for the CsI solutions E, F and G over the range 0.005 $pm^{-1} \leqq s \leqq 0.16\ pm^{-1}$: the distance r (pm), the temperature factor $10b$ (pm^2), the number of interactions n, and parameters R (pm) and $10B$ (pm^2) defined in (3) in the text. The parameter values were used in the theoretical curves in Fig. 2.

		E 2.78 molal 293 K	F 2.78 molal 343 K	G 5.56 molal 343 K
Cs–O	r	300.6(4)	305.6(4)	302.2(2)
	$10b$	17.0(9)	23.1(8)	11.5(2)
	n	5.75(6)	4.73(5)	3.04(2)
I–O	r	367.2(5)	360.4(3)	371.5(1)
	$10b$	28(1)	36.3(9)	29.7(3)
	n	7.2(1)	8.22(7)	6.80(3)
Cs–I	r	388.2(9)	384.9(5)	384.7(2)
	$10b$	61(3)	51(1)	73.1(5)
	n	0.80(1)	0.81(1)	1.177(5)
O–O	r	280(2)	280.1(6)	280.0(6)
	$10b$	6(2)	5(1)	1.2(6)
	n*	1.00(4)	1.53(3)	0.86(2)
Cs	R	348(2)	356(2)	349(1)
	$10B$	30(10)	44(6)	31(2)
I	R	482(7)	513(4)	503(2)
	$10B$	1440(70)	520(40)	670(20)
H	R	269(4)	301(6)	285(4)
	$10B$	70(30)	170(30)	200(200)
O	R	316(1)	306(1)	310(1)
	$10B$	33(4)	141(6)	163(5)

* Per H_2O molecule.

This is partly because the water content in the CsI solutions decreases with increasing ion concentration, and no sufficient water molecules are available to form the separate hydration shells of Cs^+ and I^-. Another reason may be due to the formation of the contact Cs^+-I^- ion-pairs, which prevent water molecules from contacting with Cs^+ in the direction along the Cs^+-I^- bond. The Cs–O distance obtained in the present study is slightly smaller than that (322 pm) obtained in an MD simulation of a 2.2 molal CsF solution [16], but reasonably agrees with the previous X-ray diffraction results (313–315 pm) [14, 31].

3.5. I^- Hydration in LiI Solutions

As seen in Table 2, the I–O distance does not change significantly with concentration and the temperature. Table 4 summarizes the parameter values on the hydration structure of I^- ion previously reported. The I–O distance obtained in the present study is in good agreement with most of the previous results within experimental uncertainties.

When the ion concentration increased, the average coordination number in the first hydration shell of I^- significantly decreased, which agreed with the previous findings [14, 15]. This result is expected from the weak hydration of I^-. On the other hand,

Table 4. Comparison of the results on the hydration structure of I^- obtained with the X-ray diffraction method by various authors. M and m stand for molar and molal concentrations, respectively. The interatomic distance r_{IO}, the temperature factor $10b$ which relates to the root-mean-square deviation l by $b = \frac{1}{2}l^2$, and the number of interactions n_{IO} are given here.

Solute	r_{IO}/pm	$10b$/pm^2	n_{IO}	Concentration	Temperature/K	Ref.
LiI	365–369	–	9.4–6.7	2.5–5.0 m	298	14
NaI	376	–	8.9–6.1	10 m	298	14
NH_4I	361	28.8	6	[a]	298	26
LiI, KI	370	–	9.6–4.2	0.4–4.6 M	298	15
NaI	360	40	6	7 M	298	27
LiI	363	33.8	6.9	2.2 m	298	29
LiI	358	46	8.3	2.78 m	293	This work
LiI	358	34	7.7	2.78 m	343	This work
LiI	355	19	5.6	6.05 m	293	This work
LiI	359	16	4.7	6.05 m	343	This work
CsI	367	28	7.2	2.78 m	293	This work
CsI	360	36	8.2	2.78 m	343	This work
CsI	372	30	6.8	5.56 m	343	This work

[a] $[H_2O]/[NH_4I] = 8$.

the temperature factor for the $I^- - H_2O$ interactions decreased with increasing ion concentration. According to the MD simulations, the number of the nearest neighbour water molecules at halide ions widely spreads from, for instance, 3 to 12 [34], the average number of the spread values being defined as the hydration number of the halide ion according to the definition in the X-ray diffraction method. The large temperature factor of the $I^- - H_2O$ interactions in the 2.78 molal solution may be caused by a wide variety of the I–O distances in the hydration shell of I^- ions with various hydration numbers. As the hydration number of I^- decreases with increasing concentration of LiI, a narrower distribution of the hydration numbers of each iodide ion should result, which leads to more or less similar I–O distances within the hydration shell.

When the hydrogen bonded water structure in the bulk is broken at a high temperature, the hydration structure of I^- may be relatively enhanced. In fact, the cross-over temperature, at which the negative hydration of an ion changes to the positive one, has been reported to be 334–348 K [6, 35]. The n_{OO} values given in Table 2, which decrease with increasing temperature, show that appreciable amounts of hydrogen bonds in solutions B and D are broken at 343 K. The relatively enhanced hydration structure of I^- at an elevated temperature may result in a smaller value of the mean-square-root of the distributed I–O distances than that at lower temperature.

3.6. *I^- Hydration in CsI Solutions*

The I–O distance in the hydration shell of I^- agrees well with that observed by X-ray investigations on aqueous solutions containing iodide ions [14, 15, 27].

The average coordination number of I^- found in the CsI solutions did not change significantly with increasing concentration and temperature. This is in contrast to the findings for aqueous LiI solutions, in which the average coordination number of I^- decreases with an increase in the ion concentration and temperature. These different trends in the average coordination numbers of I^- in the CsI and LiI solutions may not be discussed simply on the basis of a counter ion effect due to different ioinic sizes, since ion-pair formation occurs in the CsI solutions. Another practical reason may be due to the least-squares calculations, in which the I–O distance is close to the Cs–I distance and their structural parameter values are strongly correlated. This problem has been overcome in an MD simulation of aqueous CsI solutions at different ion concentrations and temperatures [36], which gives partial pair correlation functions.

As is seen in Table 3, the number of $H_2O - H_2O$ interactions is small in comparison with the $n_{OO} = 2$ in pure liquid water having a tetrahedral network [30], thus indicating that the nearest-neighbour $H_2O - H_2O$ interactions are not significant in the present solutions. This may be expected from the structure breaking property of the large Cs^+ and I^- ions from the high solute concentrations.

3.7. *$Cs^+ - I^-$ Ion-Pairs*

The Cs–I distance has converged to 385 pm on the average for the three CsI solutions. The number of $Cs^+ - I^-$ interactions was larger than 0.8, indicating that about 80% of the ions contacts each other. The n_{CsI} value seemed to increase with increasing temperature and was larger than unity for the 5.56 molal CsI solution. This indicates an appreciable amount of aggregates formed in the solution and it may be concluded that the broad peak observed at 600–800 pm in the RDF of the 5.56 molal solution originates from the ion-ion interactions within the aggregates. This conclusion is also supported by the enhanced Cs–I peak, as seen in the DRDFs (Figure 3).

The formation of such aggregates suggests that they may be regarded as *embryos*, in the crystallization process. In order to further examine the three-dimensional structure of the aggregates, which is difficult to obtain by the X-ray diffraction measurements, we have performed an MD simulation of aqueous CsI solutions with the same composition as in the present measurements, the results of which will be published elsewhere [36].

4. Concluding Remarks

X-Ray scattering experiments of aqueous CsI and LiI solutions with different solute concentrations and temperatures have demonstrated a structural change of the hydration shell of I^-. The hydration structure of Cs^+ is rather sensitive to changes in temperature and concentration, and the average coordination number of the Cs^+ ion decreases with

increasing concentration and temperature. On the contrary, the hydration structure of I^- does not change significantly with increasing concentration and temperature in the CsI solutions. With an increase in concentration and temperature, the H_2O-H_2O bonds are broken to a considerable extent. The Cs^+-I^- ion-pair formation has been verified from the measurements of the 2.78 and 5.56 molal aqueous CsI solutions. Ionic aggregation with increasing concentration is suggested.

Acknowledgement

The present work has been financially supported by the Grant-in-Aid for Special Project Research No. 61134043 from the Ministry of Education, Science and Culture. For a part of the calculations the HITAC M-280H computers at the Institute for Molecular Science at Okazaki and National Laboratory for High Energy Physics at Tsukuba were used.

[1] J. E. Enderby and G. W. Neilson, Rep. Prog. Phys. **44,** 595 (1981) and references therein.
[2] K. Heinzinger, Pure Appl. Chem. **57,** 1031 (1985), and references therein.
[3] V. I. Ionov and R. K. Mazitor, Zh. Strukt. Khim. **9,** 895 (1968).
[4] L. Endom, H. G. Hertz, B. Thül, and M. D. Zeidler, Ber. Bunsen. Phys. Chem. **71,** 1008 (1968).
[5] B. C. Krumgal'z, Zh. Strukt. Khim. **13,** 592 (1972); Zh. Strukt. Khim. **13,** 774 (1972).
[6] G. A. Krestov and V. K. Abrosimov, Zh. Strukt. Khim. **8,** 822 (1967).
[7] H. Rüterjans, F. Schreiner, U. Sage, and T. Ackermann, J. Phys. Chem. **73,** 986 (1969).
[8] P. S. Leung and G. J. Safford, J. Phys. Chem. **74,** 3696 (1970).
[9] A. F. Borina and O. Ya. Samoilov, Zh. Strukt. Khim. **8,** 817 (1967).
[10] M. N. Buslaeva and O. Ya. Samoilov, Zh. Strukt. Khim. **2,** 551 (1961).
[11] Gy. I. Szász and K. Heinzinger, Earth and Planetary Science Letters, **64,** 163 (1983).
[12] L. G. Sillén and A. E. Martell, Ed., Stability Constants, Spec. Publ., No. 17, 1964; Supplement No. 1, Spec. Publ. No. 25, The Chemical Society, London 1971.
[13] E. Högfeldt, Ed., Stability Constants of Metal-Ion Complexes, Part A, Pergamon Press, 1982.
[14] R. M. Lawrence and R. F. Kruh, J. Chem. Phys. **47,** 4758 (1967).
[15] M. Ya. Fishkis and T. E. Soboleva, Russ. J. Struct. Chem. **15,** 175 (1974).
[16] Gy. I. Szász and K. Heinzinger, Z. Naturforsch. **38a,** 214 (1983).
[17] K. Ichikawa, T. Kameda, T. Matsumoto, and M. Misawa, J. Phys. C: Solid State Phys. **17,** L725 (1984).
[18] A. P. Copestake, G. W. Neilson, and J. E. Enderby, J. Phys. C: Solid State Phys. **18,** 4211 (1985).
[19] P. Bopp, I. Okada, H. Ohtaki, and K. Heinzinger, Z. Naturforsch. **40a,** 116 (1984).
[20] K. Tanaka, N. Ogita, Y. Tamura, I. Okada, H. Ohtaki, G. Pálinkás, E. Spohr, and K. Heinzinger, Z. Naturforsch. in press.
[21] Y. Tamura, I. Okada, H. Ohtaki, K. Tanaka, N. Ogita, and K. Heinzinger, Z. Naturforsch., to be published.
[22] H. Ohtaki, M. Maeda, and S. Itoh, Bull. Chem. Soc. Japan **47,** 2217 (1974); H. Ohtaki, T. Yamaguchi, and M. Maeda, Bull. Chem. Soc. Japan **49,** 701 (1976).
[23] T. Yamaguchi, G. Johansson, B. Holmberg, M. Maeda, and H. Ohtaki, Acta Chem. Scand. **A38,** 437 (1984).
[24] International Tables for X-Ray Crystallography, Vol. IV, Kynoch Press, Birmingham 1974.
[25] G. Johansson and M. Sandström, Chem. Scr. **4,** 195 (1973).
[26] A. H. Narten, J. Phys. Chem. **74,** 765 (1970).
[27] M. Maeda and H. Ohtaki, Bull. Chem. Soc. Japan **48,** 3755 (1975).
[28] Gy. I. Szász, K. Heinzinger, and W. O. Reide, Z. Naturforsch. **36a,** 1067 (1981).
[29] T. Radnai, G. Pálinkás, Gy. I. Szász, and K. Heinzinger, Z. Naturforsch. **36a,** 1076 (1981).
[30] A. H. Narten, M. D. Danford, and H. A. Levy, Discuss. Faraday Soc. **43,** 195 (1973).
[31] H. Bertagnolli, J.-U. Weidner, and H. W. Zimmermann, Ber. Bunsen. Phys. Chem. **78,** 2 (1974).
[32] T. Yamaguchi, Doctoral Thesis, Tokyo Institute of Technology, 1978.
[33] Y. Tamura, T. Yamaguchi, I. Okada, H. Ohtaki, and M. Misawa, to be published.
[34] P. Bopp, I. Okada, H. Ohtaki, and K. Heinzinger, Z. Naturforsch. **40a,** 116 (1985).
[35] Yu. V. Ergin and L. I. Kostrova, Zh. Strukt. Khim. **12,** 576 (1971).
[36] Y. Tamura, T. Yamaguchi, I. Okada, and H. Ohtaki, to be published.